

NASA/TM—2008-215262



# Signal Detection Theory Applied to Helicopter Transmission Diagnostic Thresholds

*Paula J. Dempsey*  
*Glenn Research Center, Cleveland, Ohio*

*Jonathan A. Keller and Daniel R. Wade*  
*U.S. Army, Redstone Arsenal, Alabama*

## NASA STI Program . . . in Profile

Since its founding, NASA has been dedicated to the advancement of aeronautics and space science. The NASA Scientific and Technical Information (STI) program plays a key part in helping NASA maintain this important role.

The NASA STI Program operates under the auspices of the Agency Chief Information Officer. It collects, organizes, provides for archiving, and disseminates NASA's STI. The NASA STI program provides access to the NASA Aeronautics and Space Database and its public interface, the NASA Technical Reports Server, thus providing one of the largest collections of aeronautical and space science STI in the world. Results are published in both non-NASA channels and by NASA in the NASA STI Report Series, which includes the following report types:

- **TECHNICAL PUBLICATION.** Reports of completed research or a major significant phase of research that present the results of NASA programs and include extensive data or theoretical analysis. Includes compilations of significant scientific and technical data and information deemed to be of continuing reference value. NASA counterpart of peer-reviewed formal professional papers but has less stringent limitations on manuscript length and extent of graphic presentations.
- **TECHNICAL MEMORANDUM.** Scientific and technical findings that are preliminary or of specialized interest, e.g., quick release reports, working papers, and bibliographies that contain minimal annotation. Does not contain extensive analysis.
- **CONTRACTOR REPORT.** Scientific and technical findings by NASA-sponsored contractors and grantees.
- **CONFERENCE PUBLICATION.** Collected

papers from scientific and technical conferences, symposia, seminars, or other meetings sponsored or cosponsored by NASA.

- **SPECIAL PUBLICATION.** Scientific, technical, or historical information from NASA programs, projects, and missions, often concerned with subjects having substantial public interest.
- **TECHNICAL TRANSLATION.** English-language translations of foreign scientific and technical material pertinent to NASA's mission.

Specialized services also include creating custom thesauri, building customized databases, organizing and publishing research results.

For more information about the NASA STI program, see the following:

- Access the NASA STI program home page at <http://www.sti.nasa.gov>
- E-mail your question via the Internet to [help@sti.nasa.gov](mailto:help@sti.nasa.gov)
- Fax your question to the NASA STI Help Desk at 301-621-0134
- Telephone the NASA STI Help Desk at 301-621-0390
- Write to:  
NASA Center for AeroSpace Information (CASI)  
7115 Standard Drive  
Hanover, MD 21076-1320

NASA/TM—2008-215262



# Signal Detection Theory Applied to Helicopter Transmission Diagnostic Thresholds

*Paula J. Dempsey*  
*Glenn Research Center, Cleveland, Ohio*

*Jonathan A. Keller and Daniel R. Wade*  
*U.S. Army, Redstone Arsenal, Alabama*

National Aeronautics and  
Space Administration

Glenn Research Center  
Cleveland, Ohio 44135

---

July 2008

## Acknowledgments

The authors would like to thank the U.S. Army Black Hawk PM, Apache PM, and AMCOM G-3 CBM office located at Redstone Arsenal for their assistance and support.

Trade names and trademarks are used in this report for identification only. Their usage does not constitute an official endorsement, either expressed or implied, by the National Aeronautics and Space Administration.

*Level of Review:* This material has been technically reviewed by technical management.

Available from

NASA Center for Aerospace Information  
7115 Standard Drive  
Hanover, MD 21076-1320

National Technical Information Service  
5285 Port Royal Road  
Springfield, VA 22161

Available electronically at <http://gltrs.grc.nasa.gov>

# Signal Detection Theory Applied to Helicopter Transmission Diagnostic Thresholds

Paula J. Dempsey  
National Aeronautics and Space Administration  
Glenn Research Center  
Cleveland, Ohio 44135

Jonathan A. Keller and Daniel R. Wade  
U.S. Army  
Redstone Arsenal, Alabama 35898

## Abstract

Helicopter Health Usage Monitoring Systems (HUMS) have potential for providing data to support increasing the service life of a dynamic mechanical component in the transmission of a helicopter. Data collected can demonstrate the HUMS condition indicator responds to a specific component fault with appropriate alert limits and minimal false alarms. Defining thresholds for specific faults requires a tradeoff between the sensitivity of the condition indicator (CI) limit to indicate damage and the number of false alarms. A method using Receiver Operating Characteristic (ROC) curves to assess CI performance was demonstrated using CI data collected from accelerometers installed on several UH60 Black Hawk and AH64 Apache helicopters and an AH64 helicopter component test stand. Results of the analysis indicate ROC curves can be used to reliably assess the performance of commercial HUMS condition indicators to detect damaged gears and bearings in a helicopter transmission.

## Background

Helicopter transmission integrity is important to helicopter safety because helicopters depend on the power train for propulsion, lift, and flight maneuvering. Commercial HUMS (Health Usage Monitoring Systems) have been developed to detect damaged components using vibration based methods. Damage in helicopter transmission components produce specific fault patterns in the accelerometer vibration signatures. Various vibration signature analysis methods are developed and implemented in the commercial HUMS to detect faults in bearings, gears and shafts. Condition Indicators (CI) refer to the vibration characteristics extracted from these signatures and are used to reflect the health of the component. Numerous condition indicators are calculated from vibration data to characterize component health.

HUMS have potential for both economic and safety benefits. If component usage (cycles, load) is more severe than the design life of a component, HUMS can provide safety benefits. If component health has degraded due to anomalies

caused by harsh operational environments, limited maintenance, assembly errors, or manufacturing faults, HUMS can also provide safety benefits. If component usage is less severe, and no anomalies are detected by the HUMS system, the service life (time between component replacement or overhauls) of components may be extended. In order to identify anomalies/faults that occur in the field within a specific component, the CI must demonstrate a high level of reliability to detect anomalies/faults with minimal false alarms.

In 1999, the FAA published Advisory Circular (AC) 29-2C, Section MG-15, referred to as the HUMS AC to provide guidance for achieving airworthiness approval for a full range of HUMS applications (ref. 1). In order to receive maintenance credits to increase the service life of a specific component, the HUMS application for which credits are sought must be validated. Evidence must be provided in the form of seeded fault tests and/or fielded data that demonstrate the HUMS respond to the specific component fault with appropriate alert limits. Reference 2 provides an example of the process for obtaining maintenance credits of a helicopter transmission component.

## Threshold Assessment

Identifying a CI that reliably detects damage to specific components is required for the credit validation phase of HUMS airworthiness approval. In order to evaluate the performance of an individual CI, a threshold must be defined. Determining reliable CI threshold limits that differentiate between healthy and faulted components is necessary to ensure condition indicators effectiveness. When defining the threshold limit of a diagnostic tool, there is a tradeoff between the sensitivity of the limit to indicate damage and the number of false alarms. If a limit is decreased, damage may be detected, but more false alarms may result. If a limit is increased, false alarms may decrease, but the CI will be less sensitive to damage.

The simplest approach to set thresholds for vibration diagnostic tools is to gather baseline data under normal operating conditions, and set the threshold to values that exceed

normal operating conditions. This works well until a fault occurs and the CI value is within the normal variance for that CI across a fleet of helicopters. HUMS manufacturers have observed significant variances of CI indicator levels between healthy gearbox components (ref. 3).

Due to limited damage data on aircraft, diagnostic tools are developed in controlled ground test environments with seeded fault tests. Unfortunately, the response of the CI to a component fault in a helicopter cannot be validated until the fault occurs on aircraft. This is due to the numerous variables on aircraft that cannot be controlled or measured. The U.S. Army has undertaken a Condition Based Maintenance (CBM) program installing HUMS on fleets of helicopters. Some faults have occurred in the field when HUMS CI data has been recorded. This data will be used to validate a method of defining thresholds for transmission diagnostic algorithms that provides the minimum number of false alarms while maintaining sensitivity to transmission damage, required for HUMS performance assessment.

Receiver Operating Characteristic (ROC) curves will be used as a tool to assess the performance of different threshold values for identifying specific faults. The objective of this research is to demonstrate ROC curves developed from signal detection theory are useful analysis tools for comparing the response and performance of a CI from a healthy component to a component with a specific fault by differentiating between CI values for healthy and faulted components. CI data collected from accelerometers installed on several UH60 Black Hawk and AH64 Apache helicopters collected from two onboard commercial HUMS will be compared using ROC curves. ROC analysis will also be applied to test stand data from a commercial HUMS installed on an AH64 helicopter component test stand. Details on the ROC analysis will be discussed in the next section.

## Signal Detection Theory

Signal detection theory is an analysis technique for detecting a signal in the presence of noise. Analysis techniques can be used to improve decision making in fields where it is a challenge to discriminate between detection of an anomaly and a false alarm. There are two main components used when applying information theory to a system, information acquisition and criterion. Information acquisition refers to the data, for example CI data, available for making the decision. Criterion refers to the significant factor, for example threshold values when damage occurs, used to analyze the data (ref. 4). The criterion is a cutoff value used to detect the signal. If the CI value is larger than the criterion value, the fault is deemed present. If the CI value is less than the criterion, the component is deemed healthy.

The goal in signal detection theory is to decrease the overlap between the probability curves for healthy (noise signal) and faulted (damage signal present within the noise) condi-

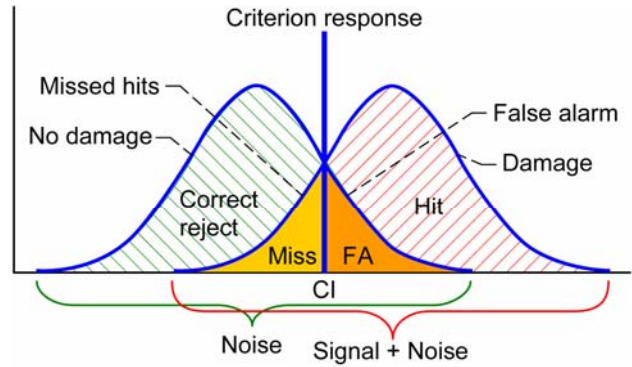


Figure 1.—Probability curves for noise and signal + noise.

tions. Statistical distributions of the healthy and faulted CI data are used to generate ROC curves. ROC curves are plotted with the false alarm rate (probability of false alarm or false positive rate) on the horizontal axis ( $x$ ) versus the hit rate (probability of detection-true alarm or true positive rate) on the vertical axis ( $y$ ). The ROC curves can be used to evaluate thresholds since they provide a visual comparison of two or more tests on common scales at all possible thresholds independent of the test scale.

Figure 1 provides a visual graph of two normal distributions for healthy and fault data for a CI. The no damage distribution is labeled “noise,” the damaged distribution is labeled “signal + noise”. The criterion line separates the graph into correct rejections, misses, false alarms and hits. The goal in signal detection theory is to decrease the noise and increase the signal strength to decrease the overlap between the two probability curves. The ability to discriminate between the healthy and faulted conditions is represented by the Discriminability Index ( $d'$ ). The discriminability index can be used to test the ability of a CI to discriminate between healthy and faulted components. CI's with higher  $d'$  values will identify clear decision thresholds.

$$d' = \text{separation/spread} = |z(\text{hit rate}) - z(\text{false alarm})| \quad (1)$$

The  $z$  refers to the  $z$  or standard score, the number of standard deviations that a given value of  $x$  is above or below the mean. The mean of the sample is equal to:

$$\bar{x} = \frac{\sum x}{n} \quad (2)$$

The standard deviation of the sample is equal to:

$$s = \sqrt{\frac{\sum (x - \bar{x})^2}{n - 1}} \quad (3)$$

Variance is equal to  $s$  squared:

$$s^2$$

Test statistic  $z$  for independent and large samples is calculated as:

$$z = \frac{x - \bar{x}}{s} \quad (4)$$

Separation corresponds to the difference between the means. The spread corresponds to the standard deviation of the probability densities. A larger  $d'$  value indicates better performance of the CI to detect healthy and faulted components.

ROC curves are used in signal detection theory to identify tradeoffs between hit rates and false alarm rates. They are used to distinguish between a signal and noise. They are used in medical fields for health decision making and to assess the predictive accuracy of the tools used to make these decisions (refs. 5 and 6). Interpretation of medical diagnostic tests can vary between diagnosticians. The ROC can be used as a tool to assess the performance of a test independent of the threshold, providing a common metric for comparison (ref. 7).

Interpretation of a signal in the presence of noise in a medical diagnostic test is comparable to predicting transmission faults based on symptoms observed in the vibration signatures. A fault produces a change in the CI levels that are compared to healthy CI levels. ROC curves can be used to summarize the accuracy of the CI to identify a specific fault. The ROC curves provide various alternatives as the criterion is moved to different levels.

The CI thresholds identified with the maximum detection capability and minimum false alarms can be integrated into health indicators. Health indicators (HI) are under development by several HUMS manufacturers (ref. 8). Health indicators provide decision making tools for the end user on the status of system health. Health indicators consist of the integration of several condition indicators into one tool that provides the health status of the component to the end user such as O.K., or needs maintenance. CI and HI performance and reliability has been difficult to evaluate due to limited failure data available to assess performance.

The advantage of using ROC curves as compared to separately viewing false alarm and damage detection rates is that the CI threshold values can be compared visually for several faulted components at all threshold values. From this information you can select the CI value with the optimal performance based on rates of false alarms and damage detection (refs. 9 and 10). ROC curves can be used to: 1) determine if a CI can discriminate between healthy and faulted component states; 2) identify CI sensitivity to damage and false alarm rate for a specific threshold value and fault; 3) quantify the effectiveness of a CI to classify a specific fault.

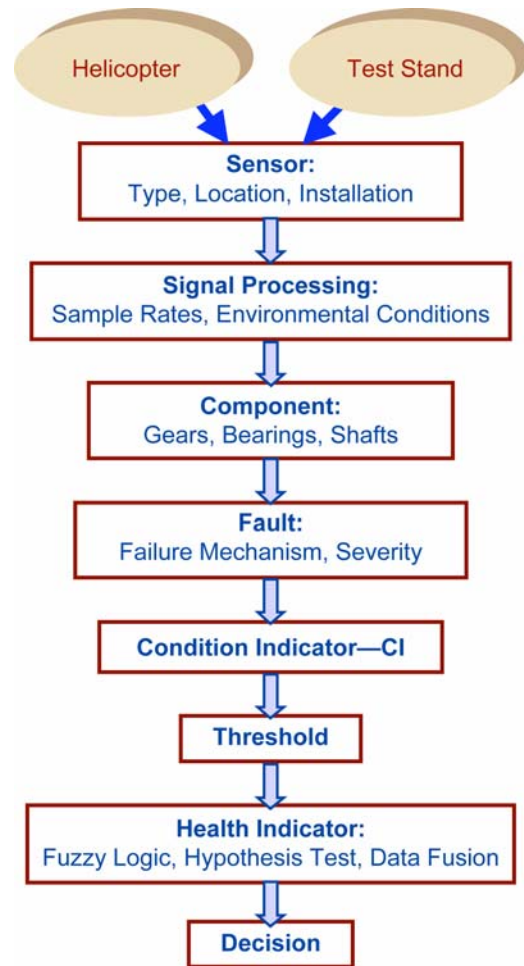


Figure 2.—Block diagram of CI/HI calculation.

Prior to identifying the steps required to generate an ROC curve for a CI, a CI must be defined to monitor a specific transmission component on a helicopter. Figure 2 provides a block diagram of this process to calculate a CI for a specific component fault. Data is collected from a helicopter or test stand using a sensor mounted at a location sensitive to the frequencies under investigation. Location and mounting can be optimized to obtain the best response, although installation is often limited to space availability on the helicopter. HUMS installation locations are correlated with components under investigation. The data acquisition system for signal processing is sampled at speeds that provide sufficient vibration data for calculating asynchronous and time synchronous averaged data based on shaft speed of components under investigation. If the CI is sensitive to environmental conditions, parameters such as torque and speed must be controlled or measured while maintaining steady flight regimes. Based on the physical phenomena of the rotating component (gears, bearings, shafts) interacting with its environment, specific fault patterns are produced in the

accelerometer vibration signatures for the component fault under investigation. The CI used is based on its sensitivity for detecting specific component faults based on analytical and experimental data.

Applying signal detection theory and the development of ROC curves requires several steps to be completed. An example of this process will be outlined. A flowchart of this process is shown in figure 3. The **first step** is to **identify a specific component, fault and CI for analysis**. The component and CI are selected if the component had a specific anomaly in the field and the CI responded. A CI is also selected if it is insensitive to operating conditions. Preliminary review of the historical monitored data should show some different responses between the healthy and faulted CI levels. **Step two** is to **calculate the CI mean and standard deviation for healthy/faulted component**. From these values, two distributions for a healthy and faulted dataset are plotted. For this demonstration, normal distributions will be used. Alternative distributions can be used for each CI. Empirical data can also be used to generate probability distributions via histograms scaled so that the area under the curve is equal to 1.

If significant overlap occurred in these two plots, this CI would not be a good choice for differentiating between a healthy and faulted component. **Step 3** is to **identify the thresholds** to use to generate ROC curves by reviewing the x axis of the distribution plots to calculate the probability of detection (hits) and probability of false alarms. **Step 4**, using the hit rate and false alarm rate, a ROC curve was generated.

In the following section, ROC curves will be developed using condition indicators measured on several UH60 Black Hawk and AH64 Apache helicopters with both healthy and faulted components. A schematic of the Black Hawk gear-box is shown in appendix A. A description of the CI used for indicating the anomalies and photos of the observed damage will be discussed. ROC analysis will also be applied to test stand data from the University of South Carolina AH64 helicopter component test stand. A summary of the datasets for analysis are shown in table 1. Although all of the datasets were analyzed, ROC curves were only generated for the highlighted datasets. In order to perform a thorough analysis of this tool, four CI datasets are required: healthy helicopter component, faulted helicopter component, healthy test stand component, faulted test stand component. To date, four complete datasets are not available for analysis. For this reason, the validation is limited to the steps required to perform this analysis on the available datasets.

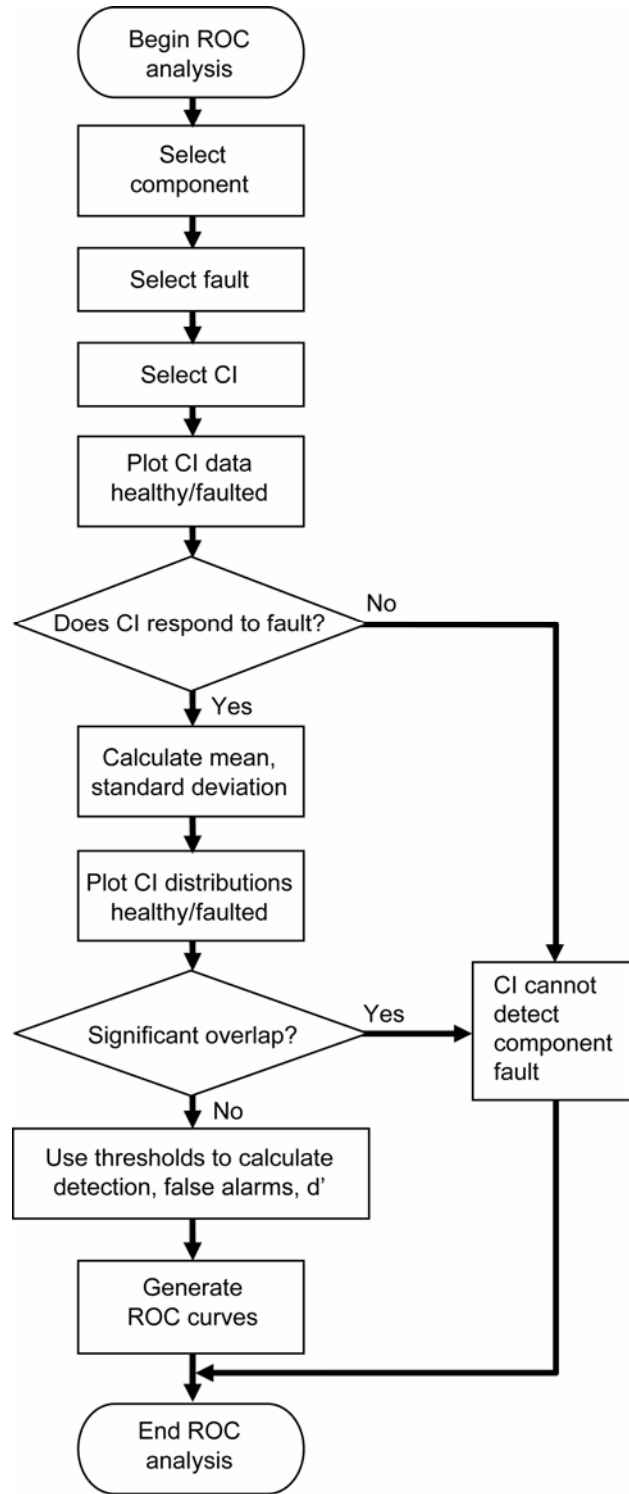


Figure 3.—Flowchart of ROC analysis.



TABLE 1.—SUMMARY OF DATASETS

Dataset timeframe	Component fault type	CI	Sensor
<i>Goodrich IVHMS</i>			
UH60 Tail 9326485 – Healthy 2/05-6/07	NA - Baseline	RK – 100t main bevel, Bearing Energies	Main Bevel left/right
UH60 Tail 9326507 – Faulted 9/06-6/07	Main Bevel <b>Gear</b> Coating Anomaly	RK – 100t main bevel	Main Bevel left/right
<i>IAC VMEP</i>			
UH60 83-23913 2/04-9/06	Tail Gearbox Output <b>Gear</b> Scoring	FM4 – Tail gearbox output gear	Tail Gearbox 19t input
UH60 83-23874 2/04-12/06	Oil cooler fan <b>bearings</b> pitting on race and cages, spalling and pitting on balls	Bearing Energy	Oil Cooler Bearing Energy
UH60 83-23900 1/04-9/07	Oil cooler fan <b>bearings</b> pitting on race and cages, spalling and pitting on balls	Bearing Energy	Oil Cooler Bearing Energy
UH60 (83-23911, 83-23845, 83-23914, 83-23921) 2/04-11/07	NA - Healthy	Bearing Energy	Oil Cooler Bearing Energy
AH64A 88-00213 – Faulted 10/05-5/07	Nose gearbox input roller <b>bearing</b> spalling on outer race and 5 rollers and cage wear	Input/Output Bearing Energy	Nose gearbox#2 input bearing
AH64D 01-05270 – Faulted 9/04-1/05	Aft hanger <b>bearing</b> spalling and corrosion pitting of single ball	Bearing Energy	Aft hanger bearing
AH64D (04-05462, 04-05464, 04-05479, 05-07005, 05-07007, 05-07009) 9/06-1/08	NA - Healthy	Fwd/Aft HB Energy	Fwd/Aft hanger bearing
<i>IAC VMEP - USC-64D-Test Stand</i>			
USC-64D TB-0001, TB-0002* 10/07	Aft Hanger <b>Bearing</b> – low grease	Aft HB energy	Aft hanger bearing
USC-64D TB-0003* 10/07-1/08	Aft Hanger <b>Bearing</b> – coarse sand con- taminated	Aft HB energy	Aft hanger bearing
USC-64D TB-0001,0002, 0003* 10/07-1/08	Fwd Hanger <b>Bearing</b> – seeded fault, 3 small pits on inner race	Fwd HB Energy	Fwd hanger bearing

\*Seeded fault

## Data Analysis

### Gears

#### UH60 Main Gearbox Bevel Gear Anomaly

CI data was collected from an onboard commercial HUMS system, Integrated Vehicle Health Management System (IVHMS), from a fleet of Black Hawk helicopters (ref. 11). A gear anomaly occurred on one helicopter, as shown in figure 4. Residual Kurtosis (RK), a gear CI, was plotted from the accelerometer located on the main bevel gear right and left output flange. The CI, referred to as RK in the IVHMS, is comparable to a more common gear CI Figure of Merit 4 (FM4). In addition, RK was also plotted for another helicopter without an anomaly.

FM4 was developed to detect changes in the vibration pattern due to damage (pitting, small, cracks) on a limited number of teeth (ref. 12). FM4 is calculated by sampling the accelerometer data and time synchronous averaging the data to shaft speed, converting the data to frequency domain, removing the gear meshing frequency, harmonics, and 1st order sidebands from the original signal, converting it back to the time domain, then calculating the fourth normalized statistical moment (normalized kurtosis) of the signal. When one or two teeth develop a defect (such as a crack or pitting) a peak or series of peaks appears in the difference signal and

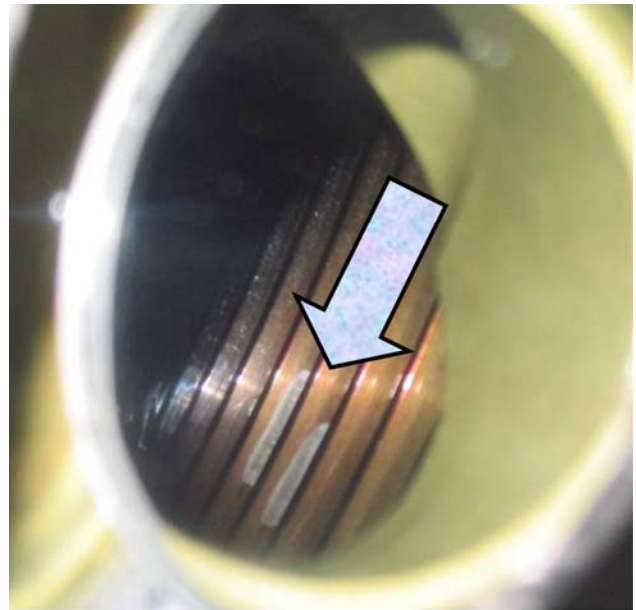


Figure 4.—UH60 main bevel gear.

FM4 reacts by increasing above this nominal value of 3. A block diagram of this calculation can be found in the appendix. Details of this CI can be found in reference (ref. 8).

Figures 5 and 6 are plots of the RK values for accelerometers installed on the main bevel gear right and left modules on both helicopters. The data is plotted versus collected data points (readings) for that helicopter. Note that the RK values for the helicopter with the gear anomaly (tail 507) are higher than the RK values measured from the helicopter with the healthy gear (tail 485). Also note RK values measured from the left accelerometer for tail 507 are higher than those measured from the right accelerometer.

Figure 7 shows the distribution of the RK values for the two accelerometers installed on the two helicopters. There is no overlap of fault and no fault data above a RK value of 4, and minimal overlap above 3.5 for the right accelerometer. Based on the mean and distribution of these two accelerometers installed on the two helicopters, the ROC curve was created and is shown in figure 8 and the data used to generate the ROC curve is shown in table 2. Based on this small dataset, values above 4 would result in no false alarms for this anomaly using CI residual kurtosis. Referring to table 2, a threshold value of 4 has the largest discriminability index.

TABLE 2.—ROC CURVE DATA FOR RK RIGHT MODULE

RK threshold	Hit rate	$z$ (hit)	False alarms	$z$ (FA)	$d'$
3	0.96	-1.8	0.27	0.6	2.4
3.5	0.84	-1	0.01	2.4	3.4
4	0.58	-0.2	0	4	4.2
4.5	0.21	0.8	0	4	3.2

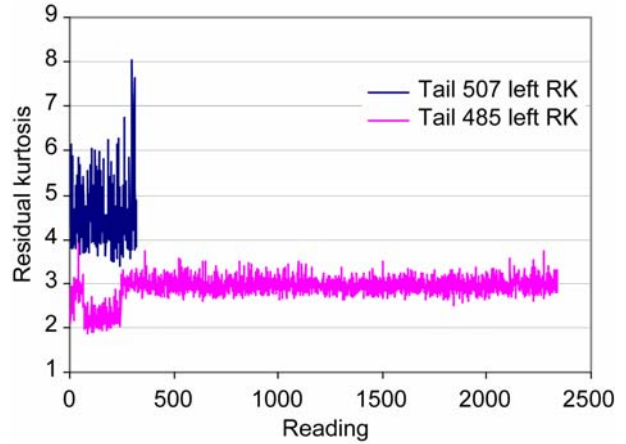


Figure 5.—Residual kurtosis for left module.

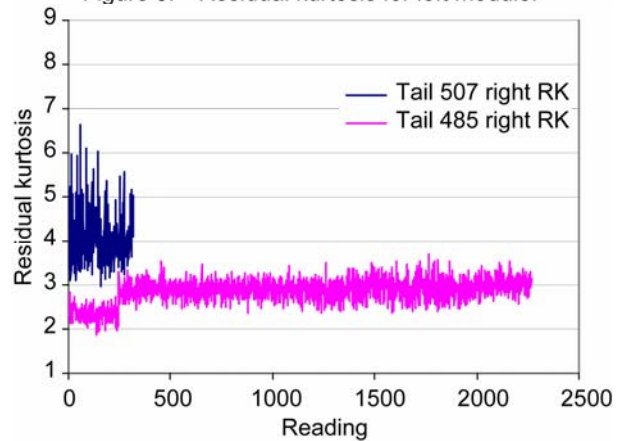


Figure 6.—Residual kurtosis for right module.

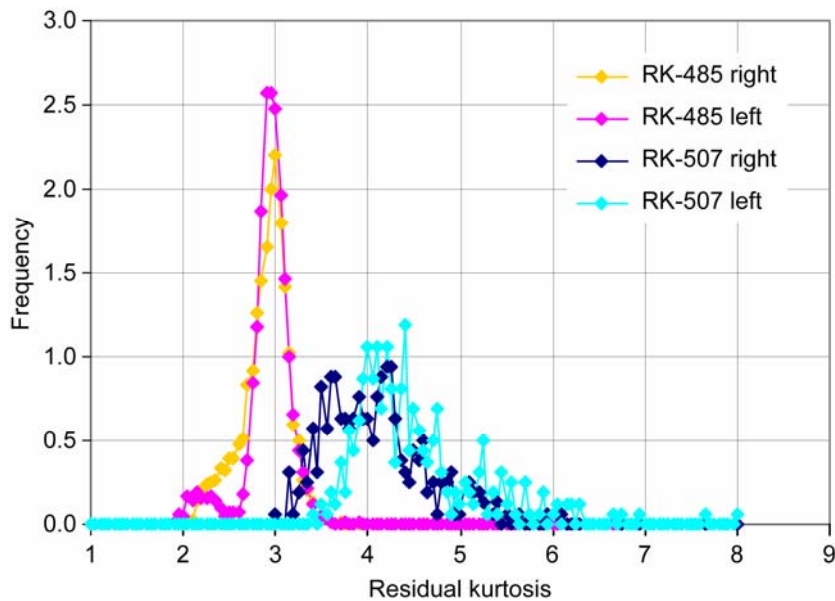


Figure 7.—Frequency plots of residual kurtosis for two helicopters.

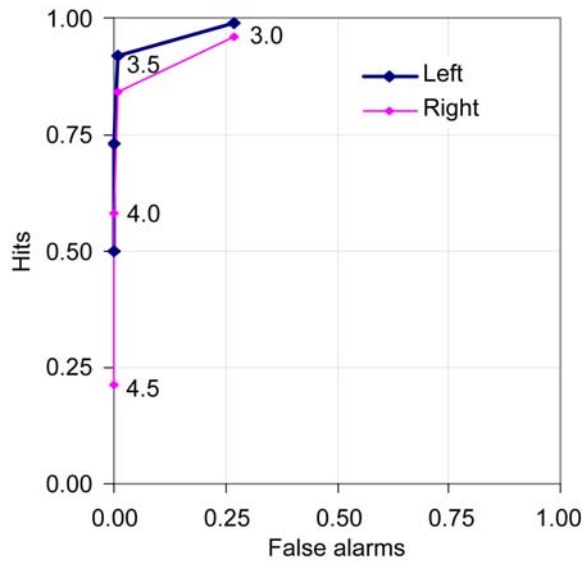


Figure 8.—ROC curves for UH60 RK data.

### ***UH60 Tail Gearbox Output Gear Anomaly***

CI data was collected from an onboard commercial HUMS system, Vibration Management Enhancement Program (VMEP) on several Black Hawk helicopters (ref. 13). A tail gearbox was removed from service due to high vibration measured by the VMEP system. Diametral scoring (fig. 9) was observed on the top land near the toe of the tail gearbox output gear. In addition, a non-magnetic wire, approximately 3-in. long, was found in the outboard (seal side) of the input bearing. The wire was protruding about ½ in. between the roller and cage near the smaller diameter and was wedged behind the rollers.

Figure 10 is a plot of the FM4 values before and after replacement. After the tail gearbox was removed and replaced, the measured vibration decreased to below 3. Due to the limited amount of data, distributions required for generating ROC curves could not be created for this dataset. However, if you look at the FM4 values before and after replacement, all of the values prior to replacement were at values above 4. The

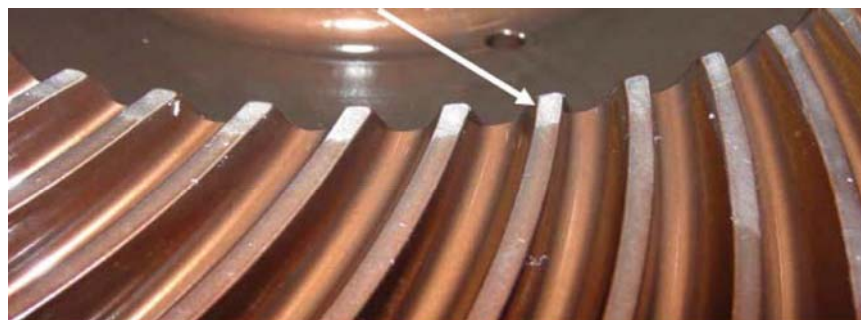


Figure 9.—Scoring damage on UH60 tail gearbox output gear.

values were under 3 when the gearbox was replaced. There is no overlap between the damaged and healthy values. A threshold of 3.5 could also be used for this geared component.

## **Bearings**

### ***UH60 Oil Cooler Fan Bearings***

CI data was collected from VMEP on two helicopters when the HUMS indicated a problem with the oil coolers at initial installation that remained for 8 months. Both oil coolers were installed in Black Hawk helicopters in the same unit and were replaced. Damage observed in the oil coolers after replacement included pitting on the races, cages, and balls of the oil cooler fan bearings. Pitting, spalling and deformation of balls were also observed. Damage to the race and balls is shown in figure 11.

Bearing Energy was the CI used to detect the oil cooler fan bearing fault. Bearing Energy is calculated as the root-sum-square (RSS) of the asynchronous vibration spectrum filtered around select frequency bands for specific bearings (ref. 13). Bearing Energy CI for the two helicopters is shown in figure 12, both before and after bearing replacement noted by the green diamond on the plot. Values exceeded 6 during time period when the components were damaged and dropped to below 4 when the bearings were replaced.

Preliminary review of the historical monitored data should show some different responses between the healthy and faulted CI levels. In order to verify the CI would not respond to healthy conditions, four helicopters in the same unit that did not experience a fault were analyzed. The oil cooler fan bearing energy CI for these four helicopters is shown in figure 13. Most values are less than the minimum faulted values, but there is some overlap with one helicopter.

The mean and standard deviation was then calculated for the Bearing Energy values when damage was present and for the four healthy helicopters. From these values two distributions for a healthy and faulted dataset were plotted and are shown in figure 14. If significant overlap occurred in these two plots, this CI would not be a good choice for differentiating between a healthy and faulted component.

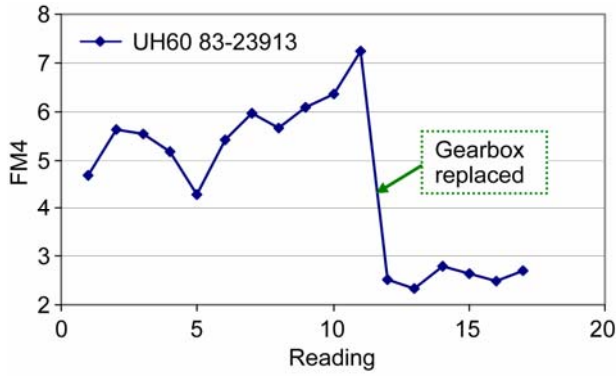


Figure 10.—FM4 values for tail gearbox.

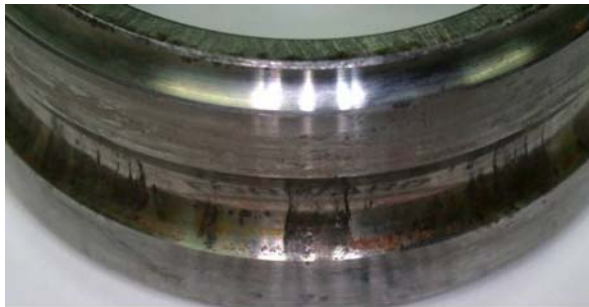


Figure 11.—Oil cooler fan bearing damage.

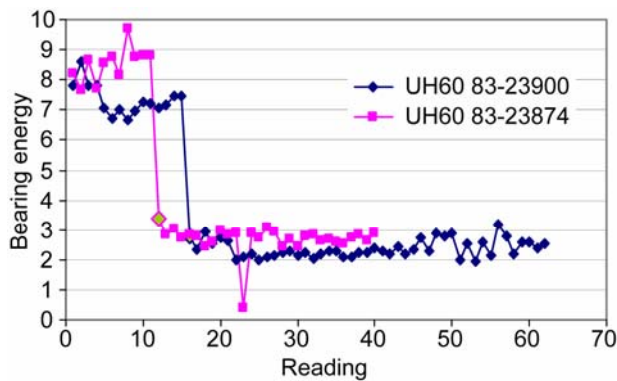


Figure 12.—Bearing energy values for oil cooler fan bearings.

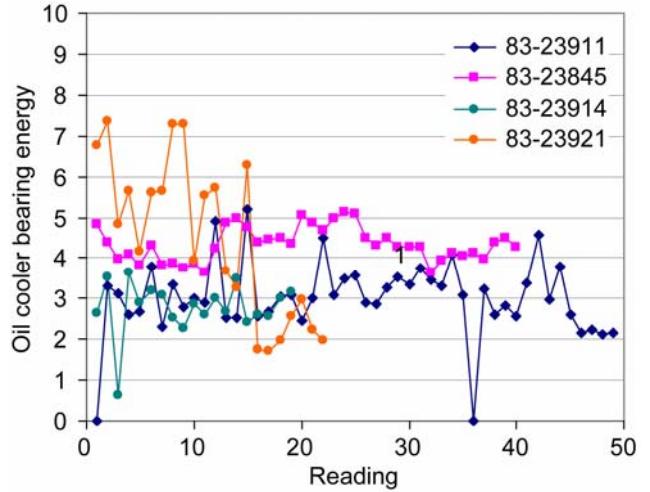


Figure 13.—Bearing energy values for 4 healthy helicopters.

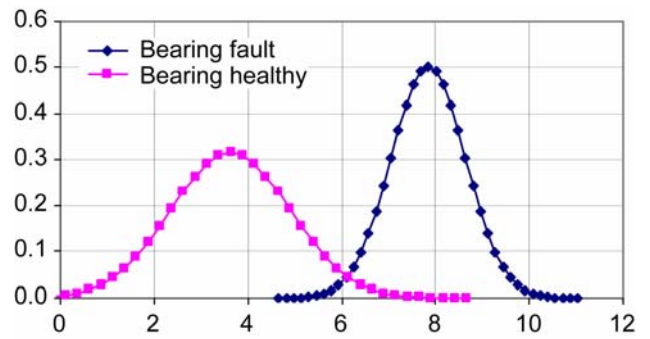


Figure 14.—Bearing energy probability curves

Threshold values used to generate ROC curves were identified by reviewing the  $x$  axis of the distribution plots. Values of 5, 6, 7, and 8 were selected. From the normal distributions and thresholds, false alarms and hit rates were calculated for bearing energy threshold values. Using the hit rate and false alarm rate, a ROC curve was plotted for this dataset and is shown in figure 15. This ROC curve shows the tradeoff between hit rates and false alarm rates based on the 4 thresholds listed in Table 3.

TABLE 3.—ROC CURVE DATA FOR BEARING ENERGY

Bearing energy threshold	Hit rate	$z$ (Hit)	FA alarms	$z$ (FA)	$d'$
5	1.00	-3.58	0.14	1.09	4.66
6	0.99	-2.32	0.03	1.88	4.20
7	0.86	-1.06	0.00	2.68	3.74
8	0.42	0.19	0.00	3.47	3.28



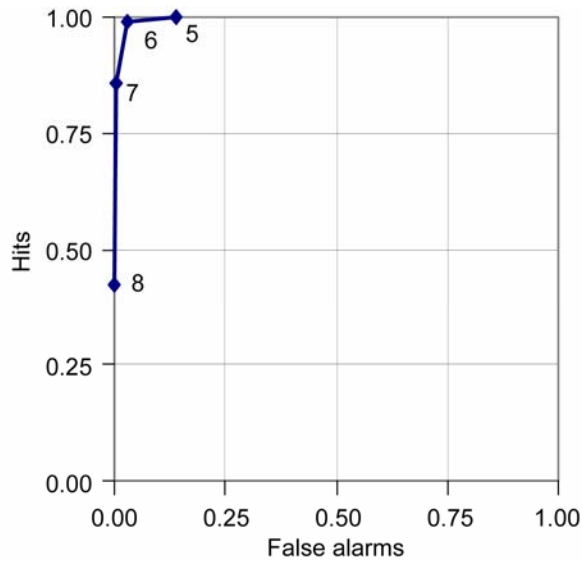


Figure 15.—ROC curves for UH60 bearing energy data.

### AH64A Nose Gearbox Bearing

CI data was collected from VMEP on a helicopter with a damaged nose gearbox input roller bearing. Spalling on the outer race, spalling on 5 rollers and cage wear was observed on the bearing. Pitting and scoring on splines of quill shaft were also observed. Damage to the outer race is shown in figure 16.

Bearing Energy Values for Nose Gearbox #2 Input Bearing are shown in figure 17. Values exceeded 6 during time period when the components were damaged and dropped to below 6 when the bearings were replaced. Due to the limited amount of data, distributions required for generating ROC curves could not be created for this dataset. However, if you look at the Bearing Energy values before and after replacement, all of the values prior to replacement were at values above 20. The values were under 7 when the gearbox was replaced. There is no overlap between the damaged and healthy values. A threshold of 7 could also be used for this geared component.



Figure 16.—Damage to the outer race.

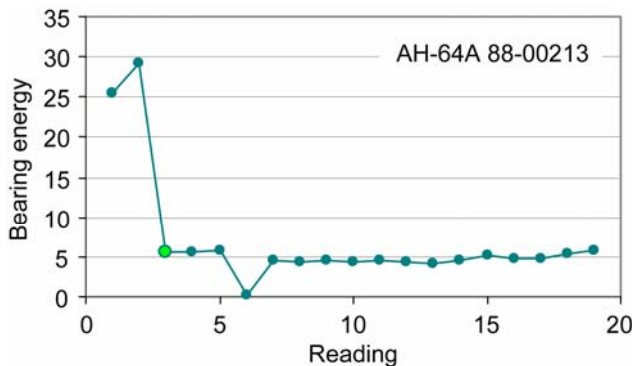


Figure 17.—Bearing energy values for nose gearbox 2 input bearing.

### AH64D Hanger Bearing

CI data was collected from a VMEP equipped helicopter when a hanger bearing was severely spalled. The bearing was removed and a new bearing reinstalled. At removal it was found that the failure was initiated by spalling and pitting of a single ball, which then caused secondary damage to the other balls and races. Bearing grease contaminated with dirt and damage to the ball is shown in figure 18.



Figure 18.—Bearing grease contaminated with dirt and damage to the ball.

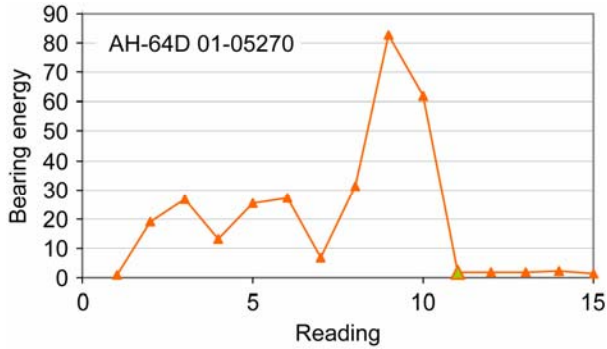


Figure 19.—Bearing energy values for aft hanger bearing.

Bearing Energy for the aft hanger bearing is shown in figure 19, both before and after bearing replacement. Values exceeded 6 during the time period when the components were damaged and dropped to below 3 when the bearings were replaced. Due to the limited amount of data, distributions required for generating ROC curves could not be created for this dataset.

### AH64D Test Stand Hanger Bearing

Tests were performed in the University of South Carolina AH64D test stand with hanger bearing faults (ref. 14). Two aft hanger bearings were tested with low grease and one aft hanger bearing was tested with grease contaminated with coarse sand. During all three tests, a forward hanger bearing with three 0.030-in. pits milled on the inner race was also installed in the test rig. The purpose of the milled pits was an attempt to generate additional spalling in the bearing over the course of the test.

Bearing Energy was the CI used to detect the faults in the forward and aft hanger bearings. Figure 20 is a plot of the aft hanger bearing energy values during the two low grease tests. Figure 21 is a plot of the aft hanger bearing energy values during the grease contaminated test. Figure 22 is a plot of the forward hanger bearing energy values measured during the three tests with the pitted bearing inner race.

In order to verify the CI response to healthy conditions, six helicopters from the same unit that did not experience tail rotor drive shaft anomalies were analyzed. The forward and aft hanger bearing energy values are plotted in figures 23 and 24 for the six helicopters. The aft bearing energy values for the low grease and the six helicopters were very similar, no significant differences were observed between CI values. But, when compared to the bearing contaminated with sand, significant differences were observed between the six healthy helicopters and the bearing contaminated with sand. The forward hanger bearing with the inner race pits is slowly increasing, but does not look significantly different than the forward hanger bearings from the six healthy helicopters.

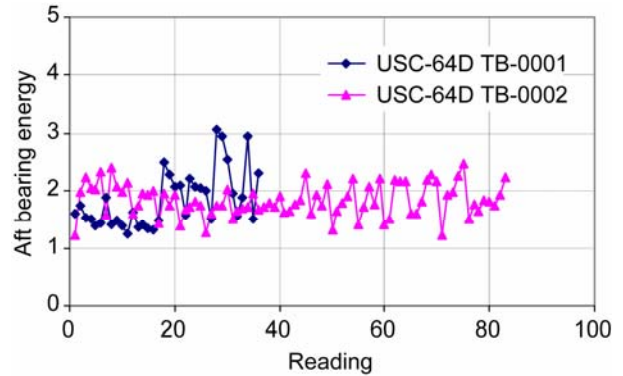


Figure 20.—Bearing energy values for low grease aft hanger bearings.

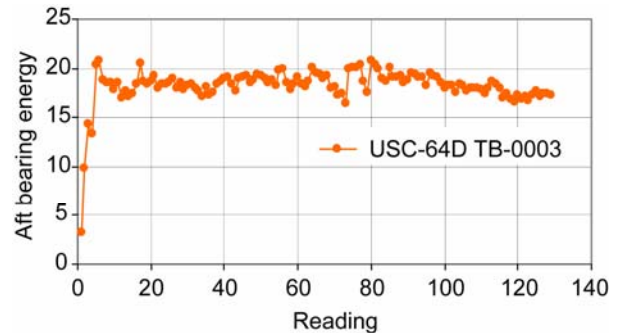


Figure 21.—Bearing energy values for coarse sand aft hanger bearing.

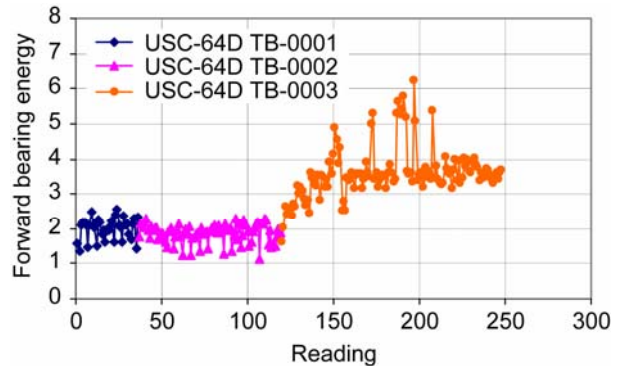


Figure 22.—Bearing energy values for pitted forward hanger bearing.

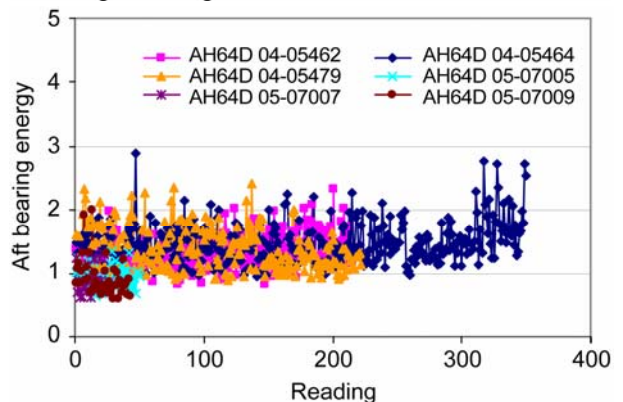


Figure 23.—Bearing energy values for aft hanger bearing.

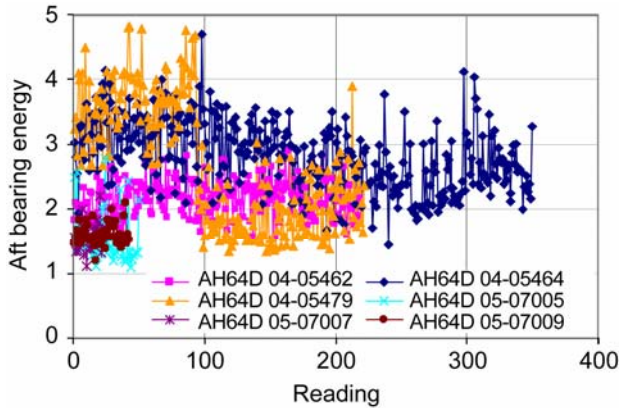


Figure 24.—Bearing energy values for forward hanger bearing.

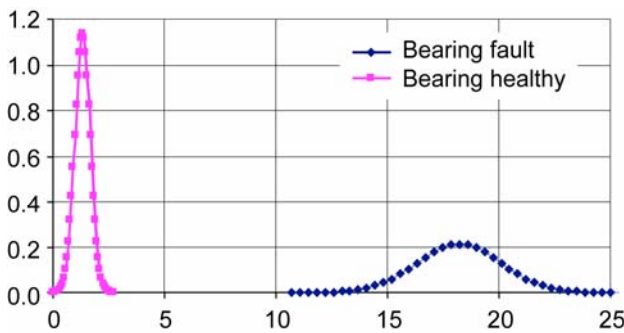


Figure 25.—Aft hanger bearing—healthy helicopter, test stand contaminated.

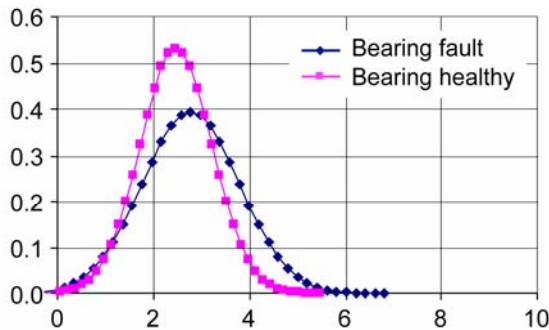


Figure 26.—Forward hanger bearing—healthy helicopter, test stand pitted inner race.

The mean and standard deviation was first calculated for the CI Bearing Energy values of the six healthy test stand aft hanger bearings and the test stand aft hanger bearings with contaminated grease. From these values two distributions for

a healthy and faulted dataset were plotted and are shown in figure 25. No overlap occurred in these two plots indicating this CI is a good choice for this type of fault. Comparing the bearing energy values for the healthy helicopter transmission and the faulted test stand, thresholds set at 5, 6, 7, and 8, used in detecting previously discussed bearing anomalies, result in 100% detection rate and 0% false alarm rate. Although enough data points were not stored when this same fault occurred in flight (see fig. 19) to generate a distribution, the mean of the dataset when damage occurred was equal to 29.56, and after replacement was 1.87 as compared to the damaged test stand mean, 18.214, and healthy helicopter mean, 1.3374.

The mean and standard deviation was then calculated for the Bearing Energy values of the six healthy test stand fwd hanger bearings and the test stand fwd hanger bearings with the pitted inner race. From these values two distributions for a healthy and faulted dataset were plotted and are shown in figure 26. Significant overlap occurred in these two plots, indicating this CI would not be a good choice for differentiating between a healthy and faulted component.

## Summary/Conclusions

The objective of this research was to demonstrate ROC curves, which are used to compare CI response between healthy and faulted components, can be used to: 1) determine if a CI can discriminate between healthy and faulted component; 2) identify CI sensitivity to damage and false alarm rate for a specific threshold value; 3) quantify the effectiveness of a CI to classify a specific fault.

CI data was analyzed from accelerometers installed on several UH60 Black Hawk and AH64 Apache helicopters collected from two onboard commercial HUMS. Data was also analyzed from a commercial HUMS installed on an AH64 test stand.

Results of the analysis indicate ROC curves can be used to assess the performance of commercial HUMS CI. Four CI datasets are required: healthy helicopter component, faulted helicopter component, healthy test stand component, faulted test stand component. To date, four complete datasets were not available. As confirmed faults are detected on HUMS equipped helicopters this analysis will continue to be validated.

Additional field data is also required to assess CI performance on different faulted components. The ROC curves can determine the probability of detection and false alarms based on a CI threshold. The ROC curves can be incorporated into health indicators that provide decision making tools for the end user on component health.





## Appendix A

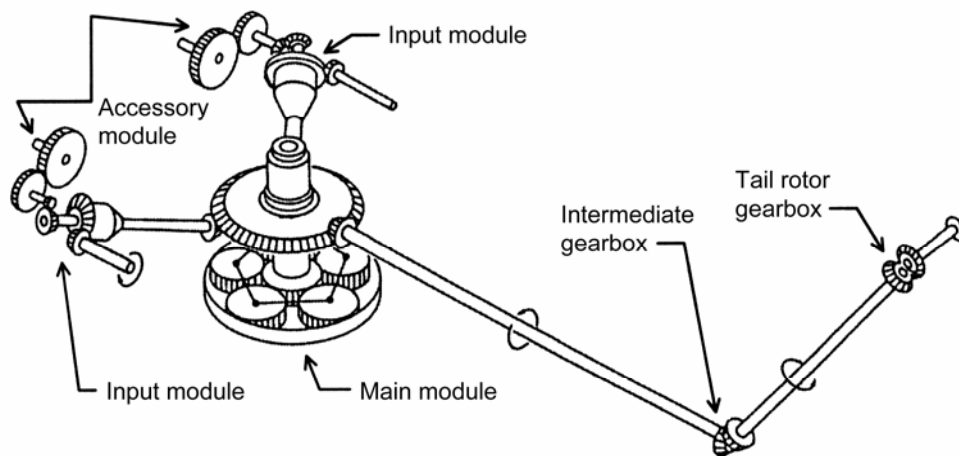


Figure A.1.—Black Hawk gearbox schematic (3400 Series) [ref. 15].



## Appendix B

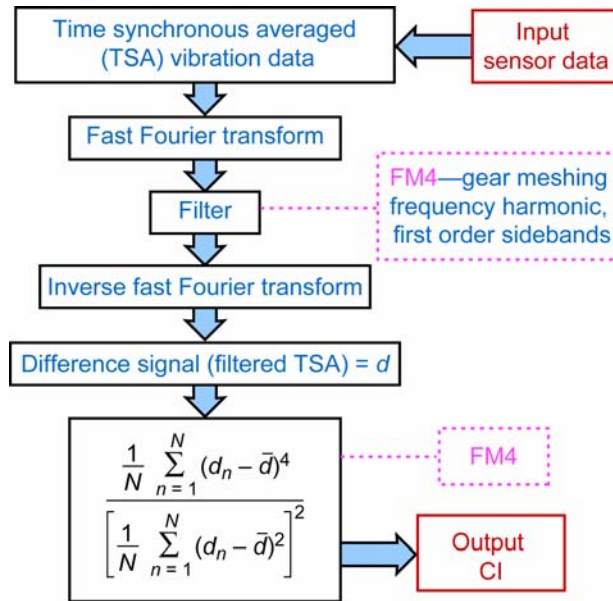


Figure B.1.—FM4 calculation.

## References

1. Federal Aviation Administration, Certification of Transport Category Rotorcraft, Ac No: 29-2C, Change: Chg 2, April 2006.
2. Suggs, D.T. and Wade, D.R. Vibration Based Maintenance Credits for the UH60 Oil Cooler Fan Assembly. Presented at the American Helicopter Society CBM Specialist Meeting, Huntsville, AL, February 2008.
3. Larder, B.D.: An Analysis of HUMS Vibration Diagnostic Capabilities. American Helicopter Society 53rd Annual Forum, May 1997.
4. Heeger, D.: Signal Detection Theory. November 12, 1997. <http://www.cns.nyu.edu/~david/handouts/sdt-advanced.pdf> accessed September 26, 2007.
5. Fawcett, T. An Introduction to ROC Analysis. *Pattern Recognition Letters* 27 (2006) 861–874. <http://www.csee.usf.edu/~candamo/site/papers/ROCintro.pdf> accessed September 26, 2007.
6. Gonen, Mithat: Receiver Operating Characteristic Curves. Paper 210-31. Proceedings of the 31st Annual SAS (SAS Institute, Inc.) Users Group International Conference. San Francisco, California March 26–29, 2006.
7. Seong Ho Park, MD, Jin Mo Goo, MD, Chan-Hee Jo: Receiver Operating Characteristic (ROC) Curve: Practical Review for Radiologists. *Korean Journal of Radiology*; March 2004; 5(1): 1–18. <http://www.kjronline.org/abstract/files/v05n01011.pdf>, accessed November 30, 07.
8. Dempsey, Paula, J., Lewicki, David, G., Le, Dy, D.: Investigation of Current Methods to Identify Helicopter Gear Health. NASA/TM—2007-214664
9. Obuchowski, N.A.: Receiver Operating Characteristic Curves in Radiology. *Radiology*, October 2003, vol. 229, no. 1.
10. Morrison, Ann Michelle. 2005. Receiver Operating Characteristic (ROC) Curve Preparation—A Tutorial. Boston: Massachusetts Water Resources Authority. Report ENQUAD 2005-20. 5 p.
11. Wright, J.: Emerging Results Using IMD-HUMS in a Black Hawk Assault Battalion. Presented at the American Helicopter Society 61<sup>st</sup> Annual Forum, Grapevine, TX, June 1–3, 2005.
12. Stewart, R.M., “Some Useful Data Analysis Techniques for Gearbox Diagnostics,” Machine Health Monitoring Group, Institute of Sound and Vibration Research, University of Southampton, Report MHM/R/10/77, July 1977.
13. Keller, J.A., Branhof, R., Dunaway, D. and Grabill, P.: Examples of Condition Based Maintenance with the Vibration Management Program. AHS 61st Forum, Grapevine, TX, June 1–3, 2005.
14. Pastides, H.: “Flying High.” Breakthrough. University of South Carolina Research and Health Sciences. Fall 2007.
15. Blunt, D.M. and Hardman, W.J.: Detection of SH-60 Helicopter Main Transmission Planet Gear Fault Using Vibration Analysis. NAWCADPAX/RTR–2000/123.

**REPORT DOCUMENTATION PAGE**

*Form Approved*  
OMB No. 0704-0188

The public reporting burden for this collection of information is estimated to average 1 hour per response, including the time for reviewing instructions, searching existing data sources, gathering and maintaining the data needed, and completing and reviewing the collection of information. Send comments regarding this burden estimate or any other aspect of this collection of information, including suggestions for reducing this burden, to Department of Defense, Washington Headquarters Services, Directorate for Information Operations and Reports (0704-0188), 1215 Jefferson Davis Highway, Suite 1204, Arlington, VA 22202-4302. Respondents should be aware that notwithstanding any other provision of law, no person shall be subject to any penalty for failing to comply with a collection of information if it does not display a currently valid OMB control number.

PLEASE DO NOT RETURN YOUR FORM TO THE ABOVE ADDRESS.

<b>1. REPORT DATE (DD-MM-YYYY)</b> 01-07-2008		<b>2. REPORT TYPE</b> Technical Memorandum		<b>3. DATES COVERED (From - To)</b>	
<b>4. TITLE AND SUBTITLE</b> Signal Detection Theory Applied to Helicopter Transmission Diagnostic Thresholds				<b>5a. CONTRACT NUMBER</b>	
				<b>5b. GRANT NUMBER</b>	
				<b>5c. PROGRAM ELEMENT NUMBER</b>	
<b>6. AUTHOR(S)</b> Dempsey, Paula, J.; Keller, Jonathan, A.; Wade, Daniel, R.				<b>5d. PROJECT NUMBER</b>	
				<b>5e. TASK NUMBER</b>	
				<b>5f. WORK UNIT NUMBER</b> WBS 659877.02.03.0550.01	
<b>7. PERFORMING ORGANIZATION NAME(S) AND ADDRESS(ES)</b> National Aeronautics and Space Administration John H. Glenn Research Center at Lewis Field Cleveland, Ohio 44135-3191				<b>8. PERFORMING ORGANIZATION REPORT NUMBER</b> E-16530	
<b>9. SPONSORING/MONITORING AGENCY NAME(S) AND ADDRESS(ES)</b> National Aeronautics and Space Administration Washington, DC 20546-0001				<b>10. SPONSORING/MONITORS ACRONYM(S)</b> NASA	
				<b>11. SPONSORING/MONITORING REPORT NUMBER</b> NASA/TM-2008-215262; AMRDEC PAO Control Number FN 3597	
<b>12. DISTRIBUTION/AVAILABILITY STATEMENT</b> Unclassified-Unlimited Subject Categories: 01, 03, and 07 Available electronically at <a href="http://gltrs.grc.nasa.gov">http://gltrs.grc.nasa.gov</a> This publication is available from the NASA Center for AeroSpace Information, 301-621-0390					
<b>13. SUPPLEMENTARY NOTES</b>					
<b>14. ABSTRACT</b> Helicopter Health Usage Monitoring Systems (HUMS) have potential for providing data to support increasing the service life of a dynamic mechanical component in the transmission of a helicopter. Data collected can demonstrate the HUMS condition indicator responds to a specific component fault with appropriate alert limits and minimal false alarms. Defining thresholds for specific faults requires a tradeoff between the sensitivity of the condition indicator (CI) limit to indicate damage and the number of false alarms. A method using Receiver Operating Characteristic (ROC) curves to assess CI performance was demonstrated using CI data collected from accelerometers installed on several UH60 Black Hawk and AH64 Apache helicopters and an AH64 helicopter component test stand. Results of the analysis indicate ROC curves can be used to reliably assess the performance of commercial HUMS condition indicators to detect damaged gears and bearings in a helicopter transmission.					
<b>15. SUBJECT TERMS</b> Rotary wing aircraft; Gears; Bearings; Health monitoring					
<b>16. SECURITY CLASSIFICATION OF:</b>			<b>17. LIMITATION OF ABSTRACT</b>	<b>18. NUMBER OF PAGES</b>	<b>19a. NAME OF RESPONSIBLE PERSON</b>
<b>a. REPORT</b>	<b>b. ABSTRACT</b>	<b>c. THIS PAGE</b>			<b>19b. TELEPHONE NUMBER (include area code)</b>
U	U	U	UU	21	STI Help Desk (email:help@sti.nasa.gov) 301-621-0390



